

Microstructure evolution of hot-rolled ODS steel during annealing

Y.B. Chun*, S.H. Kang, S. Noh, T.K. Kim

Nuclear Development Division, Korea Atomic Energy Research Institute
1045 Deadeok-daero, Yuseong-gu, Daejeon 305-353, South Korea

*Corresponding author: youngbumchun@kaeri.re.kr

1. Introduction

Oxide dispersion strengthened (ODS) steels are being developed as a cladding material for sodium-cooled fast reactors (SFR). The thermally stable oxide particles dispersed in the matrix improves the irradiation and creep resistance at high temperature [1]. As a result, ODS steels have a great potential for high burn-up and high temperature applications. General requirements for cladding material are high resistances to irradiation-induced embrittlement, void swelling, and creep, as well as a good compatibility with the molten sodium. Creep resistance at high temperature is closely related to thermal stability of microstructure, and is also affected by crystallographic texture that developed during the thermo-mechanical processes. In general, fine grain structure impairs creep resistance and strong texture leads to mechanical anisotropy. The present work investigates effects of oxide particles on thermal stability of microstructure and texture of ferritic ODS steel. For this purpose, Fe-15Cr base ferritic steel and its ODS counterpart were produced based on powder metallurgy and their microstructure were compared.

2. Methods and Results

2.1 Experimental procedures

A 15.5Cr ferritic ODS steel and its yttria-free counterpart were produced based on a powder metallurgy method. Mixtures of elemental powders with nominal compositions given in Table 1 were mechanically alloyed with a Simoloyer CM20 horizontal mill.

Table I: Chemical compositions of experimental ODS steel and its yttria-free counterpart.

	Cr	Mo	Ti	Y ₂ O ₃	Fe
ODS steel	15.5	2	0.1	0.35	Bal.
Yttria-free steel	15.5	2	0.1	-	Bal.

The mixtures of steel balls and elemental powders (steel ball to powder ratio is 15:1 in weight) were milled at 240 rpm for 48 h. The MA powders thus prepared were sealed in a mild steel container and degassed at 400°C for 1h under a vacuum of 10⁻⁴ torr. The steel containers filled with MA powders were hot-isostatically pressed (HIP) at 1150°C for 3h under 100 MPa and then hot rolled at 1150°C to a reduction in

thickness of 65%. The hot rolled plates were annealed at various temperatures between 800°C and 1450°C for 1h.

Microstructures of the annealed sample were analyzed using the electron backscatter diffraction (EBSD) technique. An EBSD analysis was undertaken using a FEI 3D Quanta field-emission-gun scanning electron microscope equipped with TSL-OIMTM data acquisition system. Samples for the EBSD analysis were mechanically ground and then further polished with alumina suspension. All the analysis made on the section normal to the transverse direction of the rolled plate. Variation of hardness with annealing temperature was determined using a Vickers micro-hardness measurement.

A small-angle neutron scattering (SANS) technique was employed to determine size distribution of oxides in the ODS steel, for which SANS facility in HANARO at Korea Atomic Energy Research Institute was used. A transverse magnetic field of 1.2 T was perpendicularly applied to the incident neutron beam to separate nuclear and magnetic scattering components. Nuclear scattering curves were extracted from a two-dimensional detector image in sectors with an azimuthal angle of 10° parallel to the applied magnetic field. Assuming that the nano-sized spherical oxides show a log-normal size distribution, the nuclear scattering curves were fitted using a SASfit program.

2.2 Results and Discussion

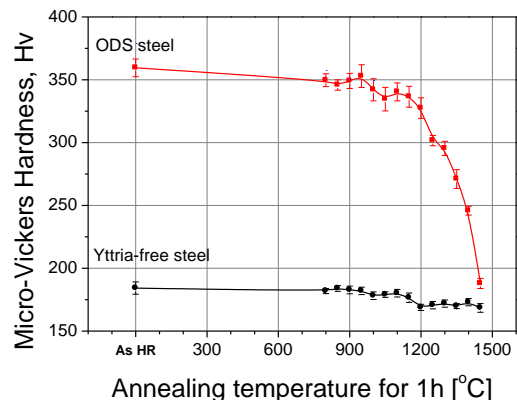


Fig. 1. Variations of Vickers micro-hardness of the hot-rolled ODS and yttria-free steels with annealing temperature.

Variation of hardness of experimental alloys with annealing temperature are shown in Fig. 1, which shows that both ODS and yttria-free steels show no significant

reduction in hardness with increasing annealing temperature up to 1100°C. The hardness of ODS steel is decreased abruptly at annealing temperatures above 1200°C, while yttria-free steel exhibits a slight reduction in hardness at temperatures up to 1450°C.

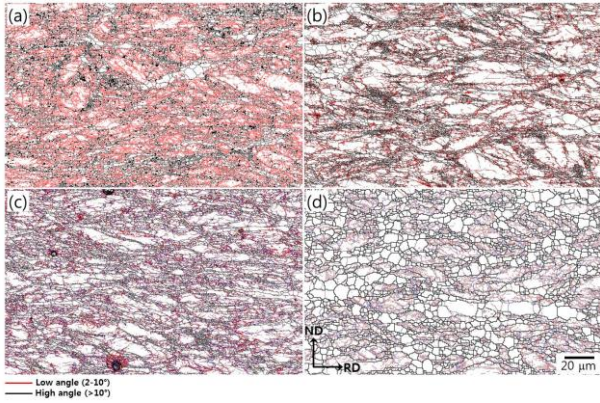


Fig. 2. Grain boundary maps of ODS steel: (a) as hot-rolled and subsequently annealed for 1 h at (b) 800°C, (c) 1300°C and (d) 1450°C.

Shown in Fig. 2 are grain boundary maps, which were obtained from EBSD measurement, of hot-rolled ODS steel during annealing. In as hot-rolled condition, fine recrystallized grains, and deformed and elongated grains co-exist in microstructure. With increasing annealing temperature up to 1300°C, more recrystallized grains form at the grain boundaries of deformed grains but their growth was suppressed. It is also observed that the density of low-angle boundaries in deformed matrix is slightly decreased with annealing temperature. When annealed at 1450°C, however, the ODS steel shows an abrupt growth of recrystallized grains.

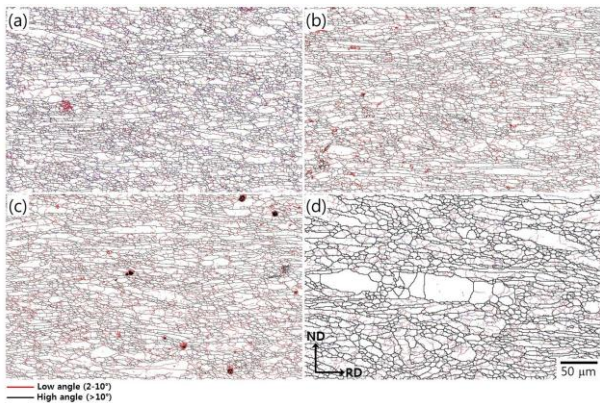


Fig. 3. Grain boundary maps of ODS steel: (a) as hot-rolled and subsequently annealed for 1 h at (b) 800°C, (c) 1300°C and (d) 1450°C.

Microstructure evolution of yttria-free steel in the as hot-rolled condition shows dynamically-recovered coarse grains and fine recrystallized grains, as shown in Fig. 3(a). With increasing annealing temperature up to 1300°C (Figs. 3(b) and 3(c)), there is no significant

change in microstructure, and grain growth is observed only for the sample annealed at 1450°C (Fig. 3(d)).

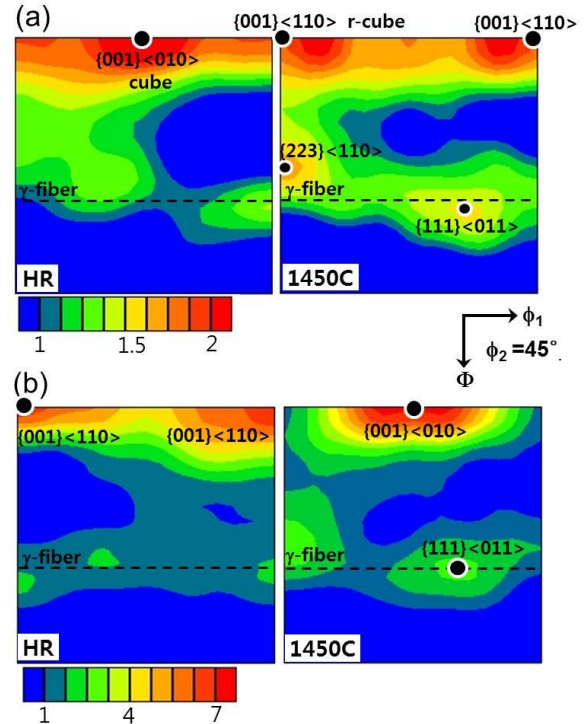


Fig. 4. $\phi_2=45^\circ$ sections of ODF for (a) the ODS steels hot-rolled and subsequently annealed at 1450°C and (b) those of yttria-free steel.

Orientation distribution functions were determined from the EBSD measurement, and the $\phi_2=45^\circ$ sections of ODF for the ODS steel and its yttria-free counterpart are presented in Fig. 4. In hot-rolled condition, the major texture components of the ODF steel are {001}<011> (cube) and γ -fiber, while those of yttria-free steel are {001}<110> (rotated-cube) and γ -fiber. When annealed at 1450°C, however, there was a change in texture: the major texture component in the ODS steel is changed to {001}<110>, whereas those in the yttria-free steel is altered into {001}<110>.

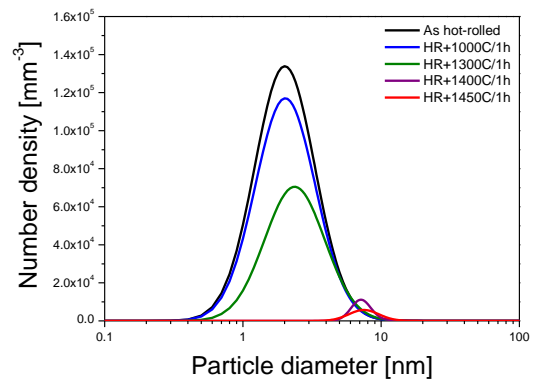


Fig. 5. Variation of the size distribution of oxide particles in the ODS steel with annealing temperature. The distributions were determined from the SANS measurement.

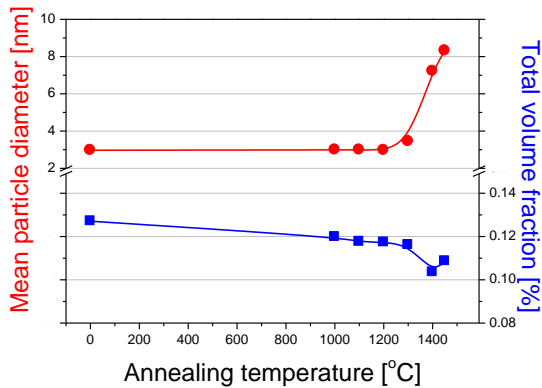


Fig. 6. Effects of Sc addition on the DBTT of the program alloys.

Thermal stability of oxide particles formed in the ODS steels were analyzed by the SANS measurement, the size distribution of the oxide particles with annealing temperature is shown in Fig. 5. It is found that oxides particles are fairly stable at temperatures up to 1200°C. When annealed at 1300°C, however, there was a slight decrease in the number density of oxide particles. Further increase of annealing temperatures up to 1450°C leads to a significant reduction in the number density of oxide particles and also to growth of the particles. The variations of mean size and total volume fraction of oxides particles are plotted against annealing temperature in Fig. 6. It is clearly shown that characteristics of oxide particles are changed abruptly at annealing temperature of 1300°C: there are dissolution and coarsening of oxide particles at annealing temperatures higher than 1300°C. Such dissolution and coarsening of oxides particles are thought to be responsible for a rapid growth of grain (Fig. 2).

3. Conclusions

The oxide particles in 15Cr ODS steel are stable at annealing temperatures up to 1200°C. However, further increase in annealing temperature results in dissolution and coarsening of oxides particles, which in turn leads to rapid growth of grains. Therefore, it is concluded that the ODS steel should be processed at temperature below 1200°C to avoid dissolution and coarsening of finely-dispersed oxide particles, and thereby to minimize loss of strength.

Acknowledgements

This work was supported by the National Research Foundation of Korea (NRF) grant funded by the Korea government (MEST) (No. 2012M2A8A1027872).

REFERENCES